Desalination and Water Treatment
www.deswater.com
doi: 10.5004/dwt.2019.24733

170 (2019) 277–286
December

Preparation of PASP/SPP hydrogels with high adsorption capacity for Pb(II)

Hao Wang*, Li Wang

College of Material Science and Art Design, Inner Mongolia Agricultural University, Hohhot 010018, China, emails: 329440666@qq.com (H. Wang), wl2083663@126.com (L. Wang)

ABSTRACT

Polyaspartic acid/salix psammophila powder (PASP/SPP) hydrogels were synthesized through aqueous polymerization and were characterized by Fourier-transform infrared spectroscopy (FTIR), X-ray diffraction (XRD), X-ray photoelectron spectroscopy (XPS) and scanning electron microscopy (SEM). The adsorption isotherms, kinetics and thermodynamics of the hydrogels for Pb^{2+} were studied. The results showed that when the pretreatment time was 15 min, the pretreatment temperature was 50°C, the concentration of $KMnO_4$ was 0.06 mol L^{-1}, the amount of PASP was 15 g, the reaction time was 3.5 h and the reaction temperature was 70°C, the adsorption capacity of the PASP/SPP hydrogel for Pb^{2+} reached the maximum 936.5 mg g^{-1}. All the adsorption processes fit very well with the Langmuir isotherm model and pseudo-second-order model. From the thermodynamic studies, the adsorption is spontaneous, exothermic and decreased randomness. The FTIR result showed that the graft copolymerization occurred between –COOH of PASP and –OH of SPP forming the PASP/SPP hydrogels. The XRD results showed that the addition of PASP destroyed the crystallinity of SPP. The SEM results showed that the surface of the PASP/SPP hydrogel was loose and porous, and after adsorption the hydrogel surface became dense. The XPS analysis proved that the Pb^{2+} ions were adsorbed on the hydrogel surface.

Keywords: Polyaspartic acid; Salix psammophila powder; Hydrogel; Adsorption; Pb^{2+}

1. Introduction

With the development of industrialization, the disordered discharge of heavy metal wastewater leads to serious environmental pollution, and heavy metal ions in wastewater are enriched through various biological chains in the water body and eventually enter into the human body, causing serious harm to human health [1]. Therefore, how to effectively treat heavy metal wastewater has become a prominent problem in the field of environmental protection.

Salix psammophila (SP) is one of the few plants that can grow in saline-alkali soil. In SP, the comprehensive cellulose content is 71.92%, the lignin content is 24.77%, and it contains active ingredients represented by hydroxyl groups [2]. Petrochemical resources are not renewable, and are now becoming less and less. SP is a renewable resource available in a large amount in nature [3,4]. Liu and Zou [5] are prepared *Salix psammophila* activated carbon (SPAC) through active pyrolysis, the static adsorption of 2,4-dichlorophenol in aqueous solutions by SPAC was studied. The results showed that the adsorption capacity is increased 3.5 times after modification. Zhang et al. [6] prepared SPAC with three different activators by chemical activation, and studied their adsorption performance for methylene blue. The results showed that the SPAC prepared by different activators had different adsorption capacity for methylene blue, of which was activated by potassium hydroxide had the largest adsorption capacity (519.63 mg g^{-1}), phosphoric acid was the second largest (347.13 mg g^{-1}) and zinc chloride was the smallest (323.45 mg g^{-1}).

Polyaspartic acid (PASP) is a kind of polyamino acid with carboxyl side chains, which naturally exists in snail and mollusc shells. Besides its water-soluble carboxylic acid properties, PASP also has strong chelation, adsorption, dispersion and other functions, and has valuable biodegradability [7,8]. At present, the research on the synthesis and properties of PASP is relatively mature, but its functional groups are relatively simple and its dispersion property is poor, which limits its applications. In order to improve this situation, PASP has been modified and compounded to prepare derivatives, which will better to solve this problem by improving

* Corresponding author.

the adsorption performance of PASP. Sun et al. [9] synthesized PASP hydrogels by using microwave method. The PASP hydrogel was an excellent adsorbent for Pb^{2+} and its adsorption capacity for Pb^{2+} was about 190 mg g^{-1}. Ye and Wang [10] synthesized PASP/lignocellulose hydrogels by an aqueous solution polymerization. The equilibrium adsorption capacities of the hydrogels for Pb^{2+} and Cd^{2+} were 980.39 and 813.01 mg g^{-1}, respectively. The adsorption capacity of hydrogel is still very high after four times of cyclic adsorption–desorption, and it is a recyclable adsorbent.

Hydrogel is a kind of hydrophilic polymer with a three-dimensional (3D) network structure. The unique structure enables it to absorb a large amount of water in a water-based environment, swell without dissolving itself, and has excellent water retention performance. The swollen hydrogel does not lose water when exposed to external pressure [11]. There are a lot of functional groups in hydrogel (such as –OH, –COOH, $–NH_2$ and $–SO_3H$), showing the advantages of high adsorption capacity, fast adsorption rate and good regenerability for the adsorption of heavy metal ions. So, hydrogel has become a hot spot in the adsorption of heavy metal ions in recent years [12].

So far, the influence of preparation conditions on the adsorption of Pb^{2+} by PASP/salix psammophila powder (SPP) hydrogels is rarely reported. Therefore, the PASP/SPP hydrogel was synthesized by aqueous solution polymerization with $KMnO_4$ as the pretreatment agent and glutaraldehyde as the cross-linking agent. The structure of the hydrogel was characterized by Fourier-transform infrared spectroscopy (FTIR), X-ray diffraction (XRD), X-ray photoelectron spectroscopy (XPS) and scanning electron microscopy (SEM). In addition, the adsorption isotherms, the adsorption kinetic models and the adsorption thermodynamics were discussed systematically.

2. Materials and methods

2.1. Materials

SPP was provided by control station of new street, Ordos, Inner Mongolia. PASP was purchased from Shandong XiYa Chemical Industry Co. Ltd., (China). Potassium permanganate and glutaraldehyde were provided by Tianjin BeiLian Fine Chemicals Development Co. Ltd.; $Pb(NO_3)_2$ (analytical grade) was purchased from Tianjin FengChuan Chemical Reagent Technology Co., China; ethylenediaminetetraacetic acid (EDTA, analytical grade) and Xylenol orange (analytical grade) and six methyl tetramine (analytical grade) were provided by Red Rock Chemical Reagent Factory in Tianjin. Hydrochloric acid was supplied by YongFei Chemical Factory in Ma Zhuang Town (China). Other reagents were used of analytical grade and all solutions were prepared with distilled water.

2.2. Characterization

FTIR spectra (Bruker-Tensor27, Germany) were taken as KBr pellets in the range of 4,000–1,000 cm^{-1}. XRD patterns (Shimadzu Analytical X-ray spectrometer, XRD-6000, Japan) were obtained using Cu Kα radiation, The XRD radiation generated at 40 kV and 30 mA, the range of diffraction angle was 0°–60°. XPS analysis of the samples was carried out using an XPS (ESCALA B21 British VG Company). Micrographs of the samples were taken using SEM (JSM-6701F, JEOL Ltd., Japan).

2.3. Preparation of PASP/SPP hydrogel

1.0 g of SPP and 50 mL of certain concentration of $KMnO_4$ solution were added to a reactor, and then it was stirred for 15 min. After 15 min, the mixture of 15 g of PASP, 1 g of glutaraldehyde and 20 mL of water was added. Then, the mixture was added into the reactor and stirred continuously for 3.5 h at 70°C. The sample was dried at a constant weight, and then the product was milled through a 200 mesh screen and used for further experiments.

2.4. Adsorption experiments

0.1 g of the PASP/SPP hydrogel was added in a 100 mL conical flask with a stopper; add 50 mL of Pb^{2+} solution with a certain initial concentration. Put the conical flask into the water-bathing constant temperature vibrator (120 rpm). In different time, temperature, pH value for adsorption, put the adsorbent from water-bathing constant temperature vibrator, when the adsorption balance was reached, then the adsorbent was separated by centrifugal machine (4,000 rpm and 5 min).

The adsorption capacity of metal ions was calculated through the following Eq. (1):

$$Q_e = \frac{(C_0 - C_e) \times V \times M}{m} \tag{1}$$

where Q_e is the amount of adsorption metal ions (mg g^{-1}) at equilibrium, C_0 is the initial moles of metal ions in solution (mol L^{-1}), C_e is the equilibrium concentration of metal ions in solution (mol L^{-1}), V is the volume of solution (mL), M is the molecular weight of metal ions (g mol^{-1}), m is the mass of adsorbent (g).

3. Results and discussion

3.1. Effect of the preparation conditions on adsorption capacity

3.1.1. Pretreatment time

As shown in Fig. 1, when the pretreatment time is 15 min, the adsorption capacity of PASP/SPP hydrogel to Pb^{2+} reached the maximum of 936.5 mg g^{-1}. At the initial stage of this reaction, the grafting increment and the molecular weight of the grafted branch chain increase rapidly, making the adsorption capacity of the hydrogel to Pb^{2+} reach the maximum. With the prolongation of pretreatment time, the active center decreased and the grafting increment decreased accordingly, resulting in the decrease of Pb^{2+} adsorption capacity of hydrogel. Therefore, the pretreatment time of 15 min is more reasonable.

3.1.2. Pretreatment temperature

As shown in Fig. 2, when the pretreatment temperature is 50°C, the adsorption capacity of PASP/SPP hydrogel to Pb^{2+}

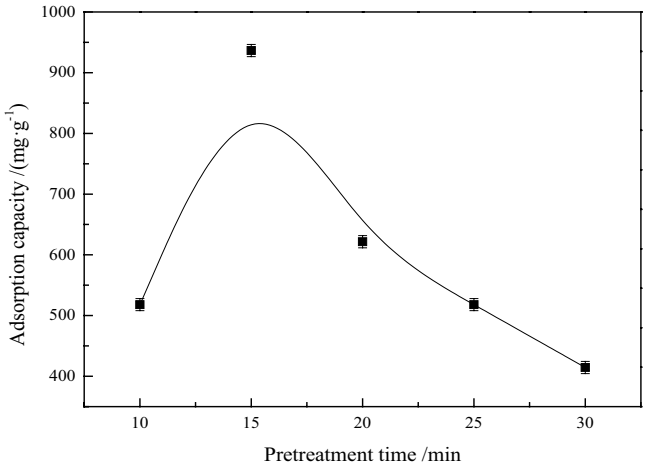

Fig. 1. Effects of the pretreatment time on the adsorption capacity of PASP/SPP for Pb^{2+}.

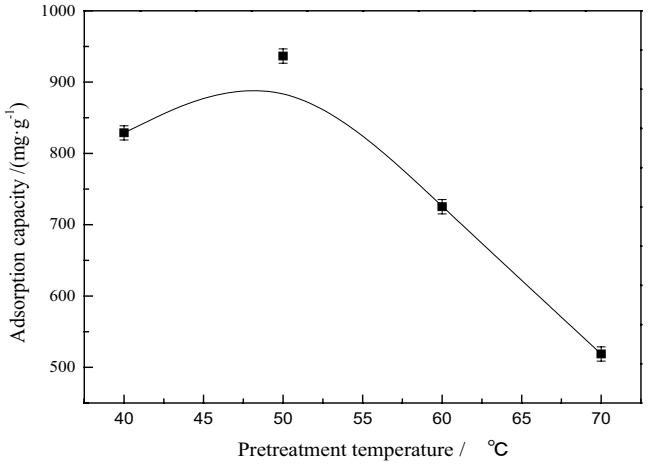

Fig. 2. Effects of the pretreatment temperature on the adsorption capacity of PASP/SPP for Pb^{2+}.

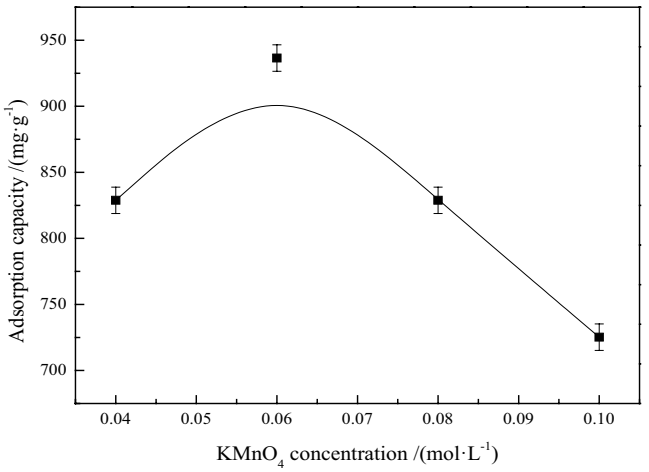

Fig. 3. Effects of the $KMnO_4$ concentration on the adsorption capacity of PASP/SPP for Pb^{2+}.

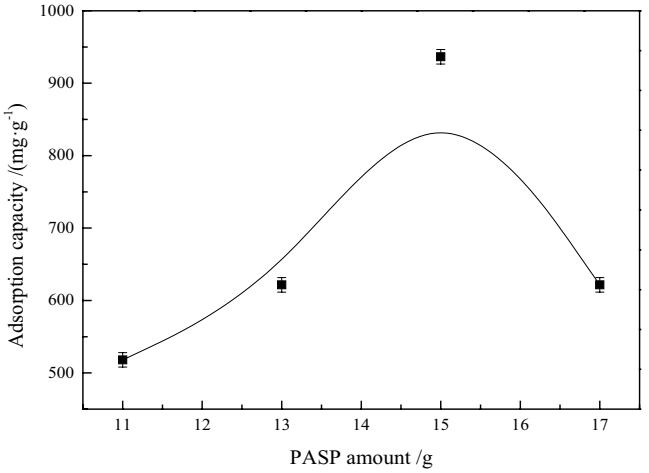

Fig. 4. Effects of the PASP amount on the adsorption capacity of PASP/SPP for Pb^{2+}.

reached the maximum of 936.5 mg g^{-1}. When the temperature is low, the decomposition rate of initiator increases and the number of chain radicals formed also increases. Therefore, the grafting rate increases with the increase of temperature, and the amount of Pb^{2+} adsorbed by hydrogel increases accordingly. However, when the grafting temperature is higher than 50°C, the transfer rate of chain free radicals to monomer and initiator increases, thus the grafting rate decreases with the increase of temperature, resulting in a decrease in the amount of Pb^{2+} adsorbed by hydrogel. Therefore, the pretreatment temperature of 50°C is more appropriate.

3.1.3. $KMnO_4$ concentration

As shown in Fig. 3, when the $KMnO_4$ concentration is 0.06 mol L^{-1}, the adsorption capacity of PASP/SPP hydrogel to Pb^{2+} reached the maximum of 936.5 mg g^{-1}. With the increase of $KMnO_4$ concentration, the number of free radicals increased, the grafting rate increased, and the amount of Pb^{2+} adsorbed by hydrogel increased. When the $KMnO_4$ concentration is too high, the free radicals generated by $KMnO_4$ on SPP increase, the reactive sites increase, and the number of grafted chains on SPP also increases, which is not conducive to the extension of grafted chains and cannot form an effective network structure, and the adsorption of Pb^{2+} on hydrogel decreases. In addition, it may be that the grafted substrate is oxidized by higher concentration of $KMnO_4$ to produce quinones with inhibition effect, resulting in the decrease of grafted quantity and finally the decrease of adsorption of Pb^{2+} on hydrogel [13]. Therefore, the $KMnO_4$ concentration of 0.06 mol L^{-1} is more appropriate.

3.1.4. PASP amount

As shown in Fig. 4, when the PASP amount is 15 g, the adsorption capacity of PASP/SPP hydrogel to Pb^{2+} reached the maximum of 936.5 mg g^{-1}. This is because with the increase of PASP amount, the collision probability between macromolecular free radicals and monomers is increased, the degree of graft copolymerization is increased, and the adsorption capacity is increased. However, with the further increase of PASP amount, SPP no longer reacts with excessive PASP,

resulting in the decrease of adsorption capacity. Therefore, it is reasonable to choose 15 g of PASP.

3.1.5. Reaction temperature

As shown in Fig. 5, when the reaction temperature is 70°C, the adsorption capacity of PASP/SPP hydrogel to Pb^{2+} reached the maximum of 936.5 mg g^{-1}. When the reaction is carried out at a lower temperature, the grafting probability of the reactants is reduced due to the weak thermal movement, and the slow polymerization reaction is not conducive to the formation of a stable 3D network structure and the adsorption capacity of the hydrogel is weak. With the increase of reaction temperature, the formed 3D network structure increases, and the adsorption capacity of hydrogel is also increases. However, when the temperature is too high, the reaction speed increases and the degree of cross-linking increases, affecting the expansion of the cross-linking network, resulting in a decrease in the adsorption capacity of the hydrogel. Therefore, the reaction temperature of 70°C is more suitable.

3.1.6. Reaction time

As shown in Fig. 6, when the reaction time is 3.5 h, the adsorption capacity of PASP/SPP hydrogel to Pb^{2+} reached the maximum of 936.5 mg g^{-1}. This is because the cross-linking network is gradually formed. With the extension of the reaction time, the formation of the cross-linking network is gradually improved and the amount of Pb^{2+} adsorbed is also increased. However, if the reaction time is too long, the cross-linking network will become excessively dense, affecting the adsorption of Pb^{2+} by functional groups, resulting in a decrease in the adsorption amount [14]. Therefore, the reaction time of 3.5 h is more reasonable.

3.2. Effect of the adsorption parameters on adsorption capacity

3.2.1. Initial concentration

As shown in Fig. 7, when the Pb^{2+} initial concentration is 0.05 mol L^{-1}, the adsorption capacity of PASP/SPP hydrogel to Pb^{2+} reached the maximum of 936.5 mg g^{-1}. This result may be attributed to the fact that with the increase in the Pb^{2+} initial concentration, the mass transfer driving force of ions has increased, thereby reducing the resistance of adsorption, meanwhile increasing the contact area between adsorbent and adsorbate, leading to increase in adsorption capacity for metal ions. When the metal ions concentration is higher than a certain value, the concentration of cations increases in the solution, which increases the competition between cations for adsorption sites, so the adsorption capacity decrease [15].

3.2.2. pH value

As shown in Fig. 8, when the solution pH value is 5.5, the adsorption capacity of PASP/SPP hydrogel to Pb^{2+} reached the maximum of 936.5 mg g^{-1}. The solution pH value is one of the parameters having considerable influence on the adsorption of metal ions because the surface charge density of the adsorbent and the charge of the metallic species present depend on

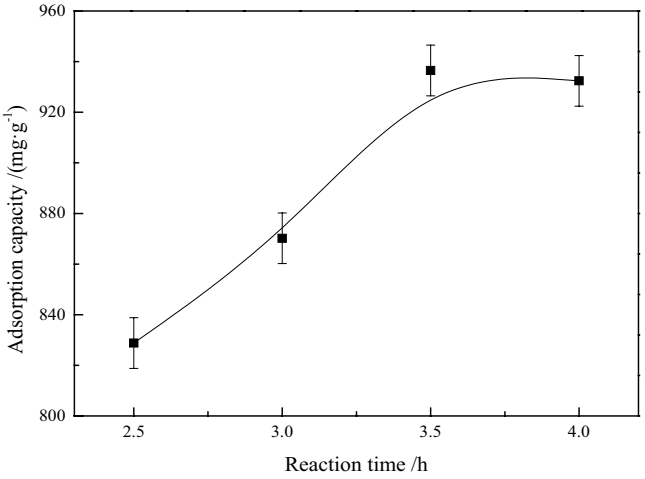

Fig. 6. Effects of the reaction time on the adsorption capacity of PASP/SPP for Pb^{2+}.

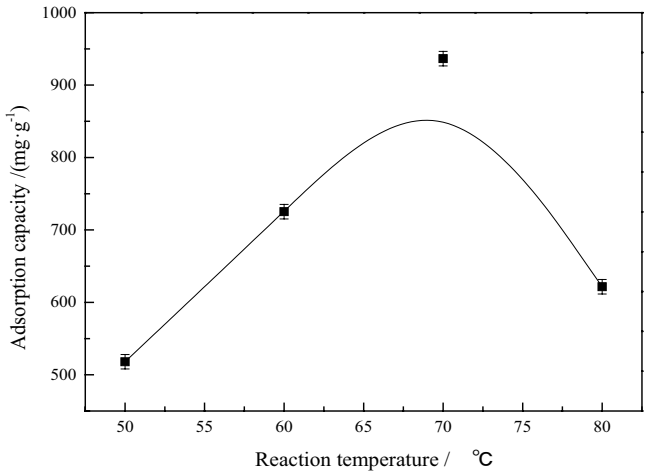

Fig. 5. Effects of the reaction temperature on the adsorption capacity of PASP/SPP for Pb^{2+}.

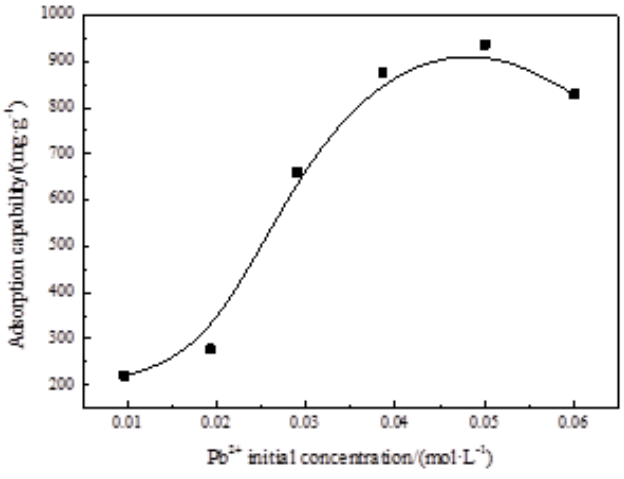

Fig. 7. Effects of the Pb^{2+} initial concentration on the adsorption capability of PASP/SPP hydrogel.

the pH value. At lower pH, a large number of H^+ compete for the adsorption sites with metal ions, which results in a low adsorption capacity. At higher pH, the competing phenomena becomes weaker, and the –COOH groups dissociate to form $–COO^-$, increasing the number of fixed ionized groups of polymer networks, leading to a high adsorption capacity. The pH value is more than 5.5, the adsorption capacity decreases lightly due to the precipitate of metal ions [16].

3.2.3. Adsorption time

As shown in Fig. 9, when the adsorption time is 30 min, the adsorption capacity of PASP/SPP hydrogel to Pb^{2+} reached the maximum of 936.5 mg g^{-1}. It can be seen that adsorption capacity of the hydrogel increased sharply in the initial stages of contact time and gradually increased with prolonging the contact time until equilibrium. It is clear that the uptake Pb^{2+} by the hydrogel was a rapid process, as it required 30 min to approach equilibrium [17]. Therefore, under our experimental conditions, the equilibrium time for the adsorption of Pb^{2+} on PASP/SPP hydrogel is 30 min.

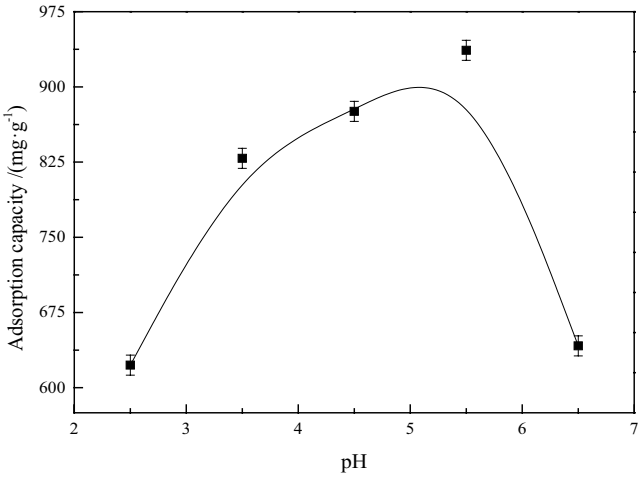

Fig. 8. Effects of the solution pH value on the adsorption capacity of PASP/SPP hydrogel.

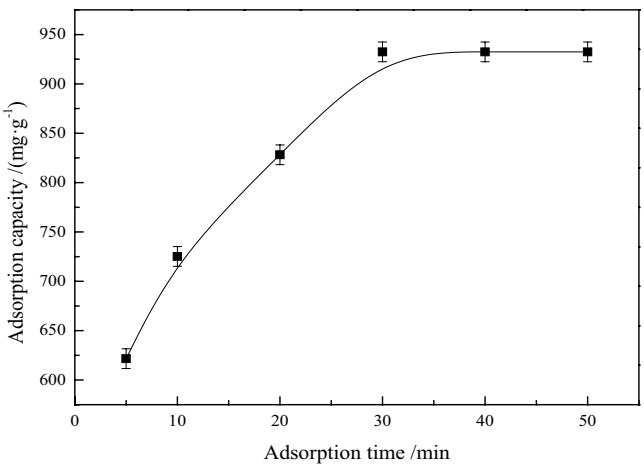

Fig. 9. Effects of the adsorption time on the adsorption capacity of PASP/SPP hydrogel.

3.2.4. Adsorption temperature

As shown in Fig. 10, when the adsorption temperature is 30°C, the adsorption capacity of PASP/SPP hydrogel to Pb^{2+} reached the maximum of 936.5 mg g^{-1}. The metal ions have higher velocity and activation energy with increasing temperature; it is easier for ions to escape from the restrictions of adsorption sites, resulting in a decrease in adsorption capacity. Besides, the adsorption is an exothermic process, the adsorption capacity decrease when the temperature increases [18], this is consistent with the results of the thermodynamics study.

3.3. Structural analysis of PASP/SPP hydrogel

3.3.1. FTIR analysis

As shown in Fig. 11, the absorption peak of SPP at 3,404 cm^{-1} is the stretching vibration peak of –OH, the absorption peak at 2,925 cm^{-1} is the stretching vibration peak of –CH, the absorption peak at 1,616 cm^{-1} is the stretching vibration peak of –COOH, and the stretching vibration peak of –C=O at 1,421 and 1,325 cm^{-1}. After graft copolymerization with PASP, the absorption peak of PASP/SPP hydrogel at 3,410 cm^{-1} increased, indicating that the number of hydroxyl groups on PASP/SPP hydrogel increased significantly; the enhancement of absorption peak at 2,915 cm^{-1} is mainly due to the introduction of long chain alkanes. The absorption peak at 1,600 cm^{-1} increased and the absorption peaks at 1,421 and 1,325 cm^{-1} decreased, indicating that graft copolymerization was developed between –COOH of PASP and –OH of SPP and formed PASP/SPP hydrogel.

3.3.2. XRD analysis

As shown in Fig. 12, the typical diffraction peaks of SPP are observed at 16.12° and 22.6°, and after grafted with PASP, the typical peak greatly weakens, the crystallinity of the

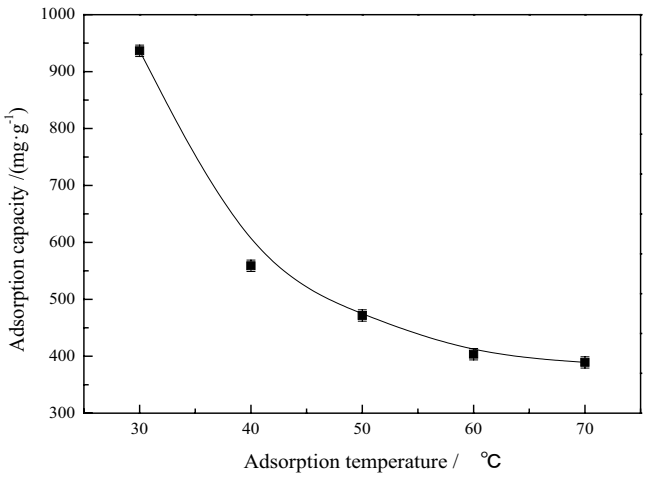

Fig. 10. Effects of the adsorption temperature on the adsorption capacity of PASP/SPP hydrogel.

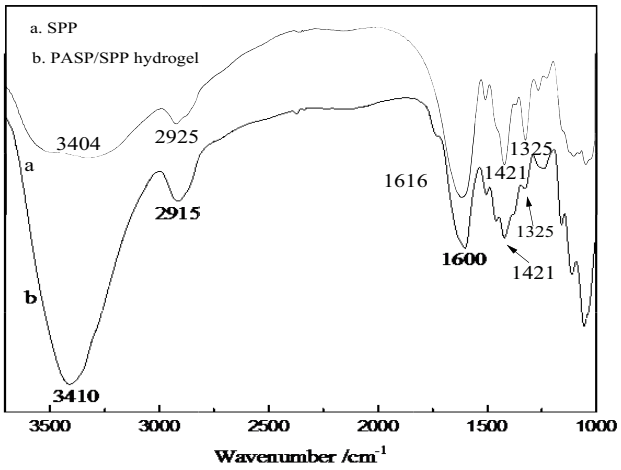

Fig. 11. (a) FTIR spectra of SPP and (b) PASP/SPP hydrogel.

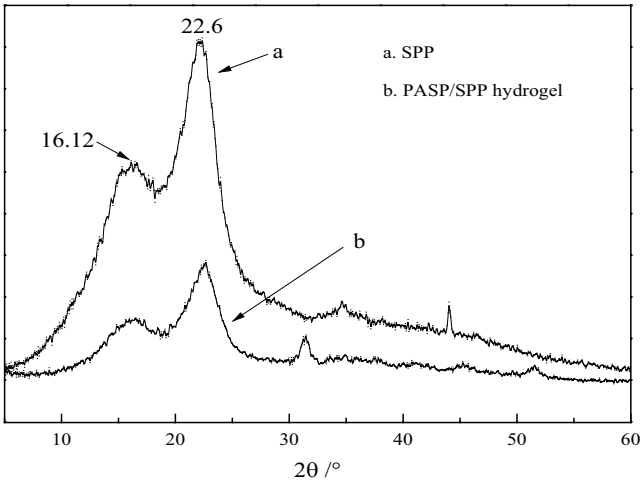

Fig. 12. (a) XRD patterns of SPP and (b) PASP/SPP hydrogel.

hydrogel decreased significantly and the amorphous region increased. This indicated that the addition of PASP destroyed the order of SPP, reduced the crystallinity and formed PASP/SPP hydrogel.

3.3.3. SEM analysis

As shown in Fig. 13, the surface of PASP/SPP hydrogel is relatively loose and porous. After adsorption of Pb^{2+}, the hydrogel surface became dense, indicating that Pb^{2+} adsorbed on the PASP/SPP hydrogel surface.

3.3.4. XPS analysis

As shown in Fig. 14, the PASP/SPP hydrogels have sharp peaks at 285, 400 and 532 eV, corresponding to C, N and O, respectively, which are the constituent elements of PASP/SPP hydrogels. After adsorbing Pb^{2+}, PASP/SPP hydrogels have new peaks at 139 eV, corresponding to the binding energy of Pb^{2+}, indicating that metal ions has been adsorbed on the active sites of hydrogels.

3.4. Adsorption isotherm model

At a certain temperature, the interaction between hydrogel and heavy metal ions can be explained by adsorption isotherms. Therefore, Langmuir and Freundlich adsorption isotherm models are selected to analyze the adsorption data of Pb^{2+} on PASP/SPP hydrogel.

Langmuir adsorption isotherm:

$$\frac{C_e}{q_e} = \frac{1}{bq_m} + \frac{C_e}{q_m} \tag{2}$$

Freundlich adsorption isotherm:

$$q_e = k_f C_e^{1/n} \tag{3}$$

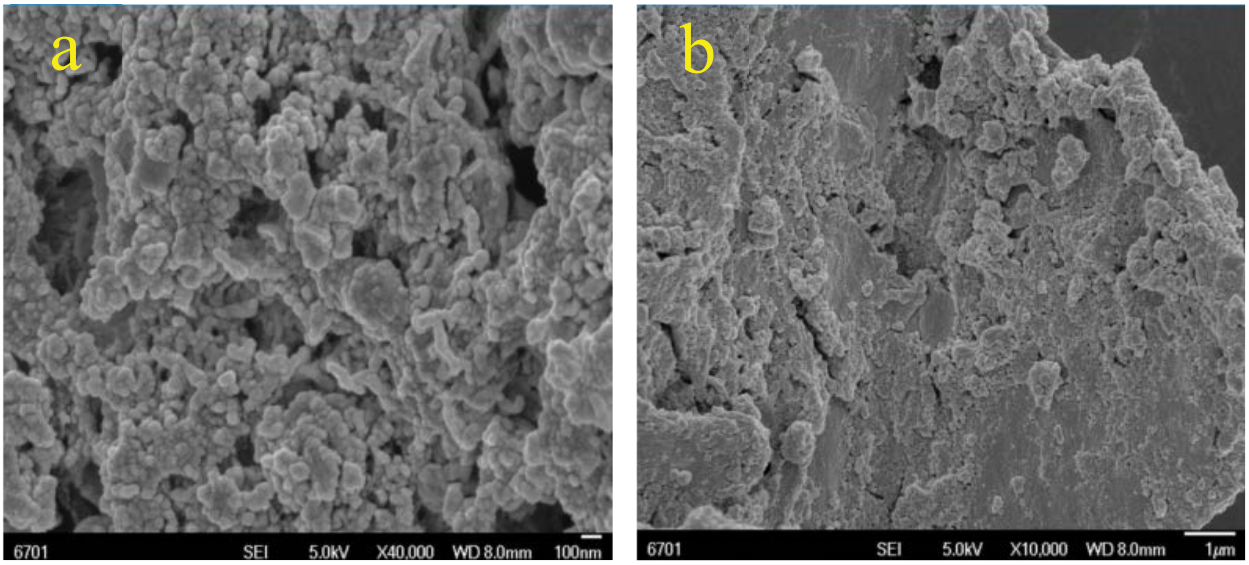

Fig. 13. (a) SEM images of PASP/SPP and (b) PASP/SPP after adsorption of Pb^{2+}.

C_e: equilibrium concentration of the solution, mg L^{-1}; q_e: equilibrium adsorption capacity, mg g^{-1}; q_m: maximum theoretical adsorption capacity, mg g^{-1}; k_f and n are Freundlich constants.

As shown in Table 1, the R^2 of Langmuir isotherm model for adsorption of Pb^{2+} by PASP/SPP hydrogel is 0.9942, and the theoretical adsorption capacity is 990.1 mg g^{-1}. According to the experimental results, the actual measured maximum adsorption capacity of Pb^{2+} by PASP/SPP hydrogel is 936.5 mg g^{-1}, and the theoretical and actual adsorption capacity is not much different, indicating that the adsorption process of Pb^{2+} by hydrogel conforms to Langmuir isotherm model. The R^2 of Freundlich isotherm model is 0.9839, and the linear correlation is not ideal. Therefore, by comparing the two adsorption isotherm models, it can be seen that the adsorption process of PASP/SPP hydrogel for Pb^{2+} meet Langmuir isotherm model and does not meet Freundlich. The adsorption process is monolayer chemical adsorption.

3.5. Adsorption kinetic model

Adsorption kinetics reflects the change of adsorption quantity with adsorption time, reveals the dynamic balance between adsorbate and adsorbent, and further better explains the adsorption mechanism. In this paper, the adsorption kinetics of PASP/SPP hydrogels are discussed by using pseudo-first-order kinetic model and pseudo-second-order kinetic model.

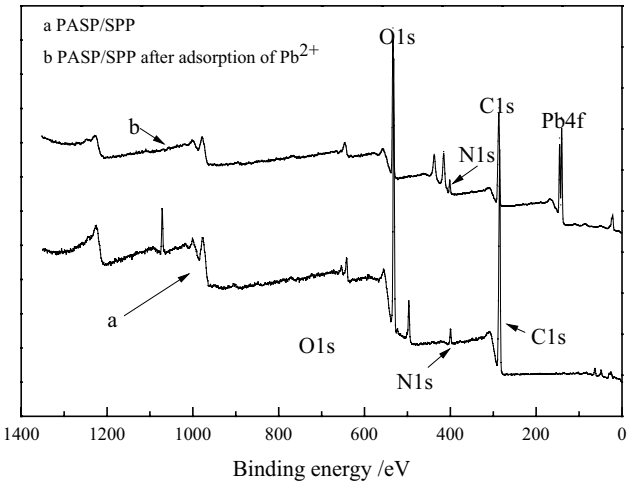

Fig. 14. (a) XPS spectra of PASP/SPP and (b) PASP/SPP after adsorption of Pb^{2+}.

Table 1
Parameters of the Langmuir and Freundlich isotherm models for the adsorption of Pb^{2+} by PASP/SPP hydrogel

	Langmuir			Freundlich		
	q_m	b	R^2	k_f	$1/n$	R^2
Pb^{2+}	990.1	0.0002	0.9942	7.6141	0.4919	0.9839

Pseudo-first-order kinetic adsorption rate equation:

$$\log(q_e - q_t) = \log(q_e) - \frac{K_1 t}{2.303} \tag{4}$$

Pseudo-second-order kinetic adsorption rate equation:

$$\frac{t}{q_t} = \frac{1}{K_2 q_e^2} + \frac{t}{q_e} \tag{5}$$

q_t: adsorption capacity at t moment, mg g^{-1}; q_e: equilibrium adsorption capacity, mg g^{-1}; K_1: rate constant of the pseudo-first-order kinetic model, min^{-1}; K_2: rate constant of pseudo-second-order kinetic model, mg g^{-1} min^{-1}.

As shown in Table 2, the R^2 of the pseudo-first-order kinetic model of adsorption of Pb^{2+} by PASP/SPP hydrogel is 0.9644, and the theoretical adsorption capacity is 454.9 mg g^{-1}. The R^2 of the pseudo-second-order kinetic model is 0.9980, and the theoretical adsorption capacity is 1006.2 mg g^{-1}. According to the experimental results, the actual maximum adsorption capacity of PASP/SPP hydrogel for Pb^{2+} is 936.5 mg g^{-1}, which is closer to the theoretical adsorption capacity of the pseudo-second-order kinetic model. Therefore, compared with the pseudo-first-order kinetics, the adsorption process of Pb^{2+} by PASP/SPP hydrogel is more in line with the pseudo-second-order kinetic model. The pseudo-second-order kinetic model is controlled by chemical adsorption mechanism, so the adsorption process of Pb^{2+} by hydrogel is mainly chemical adsorption.

3.6. Adsorption thermodynamic

Through the study of adsorption thermodynamics, we can know the extent and internal driving force of adsorption process of PASP/SPP hydrogel on metal ions, Gibbs equation and Van't Hoff equation are shown in Eqs. (6) and (7), respectively.

$$\Delta G = \Delta H - T\Delta S \tag{6}$$

$$\ln\frac{q_e}{C_e} = \frac{-\Delta H}{RT} + \frac{\Delta S}{R} \tag{7}$$

ΔG: Gibbs free energy, kJ mol^{-1}; ΔH: adsorption enthalpy, kJ mol^{-1}; ΔS: adsorption entropy, kJ mol^{-1} K^{-1}; T: adsorption temperature, K; R: ideal gas constant, 8.314×10^{-3} kJ mol^{-1} K^{-1}; q_e: liquid equilibrium adsorption capacity, mg g^{-1}; C_e: liquid equilibrium concentration, mg L^{-1}.

From Table 3, it can be seen that the adsorption enthalpy ΔH of Pb^{2+} on PASP/SPP hydrogel is –19.44 kJ mol^{-1}. $\Delta H < 0$ indicates that the adsorption of Pb^{2+} on PASP/SPP hydrogel is an exothermic reaction, which is confirmed by the increase of adsorption temperature and the decrease of adsorption

Table 2
Rate parameters of pseudo-first-order and pseudo-second-order kinetic models for the adsorption of Pb^{2+} by PASP/SPP hydrogel

	Pseudo-first-order			Pseudo-second-order		
	K_1	q_e	R^2	K_2	q_e	R^2
Pb^{2+}	0.0731	454.9	0.9644	2.9×10^{-5}	1,006.2	0.9980

amount. The adsorption entropy ΔS of PASP/SPP hydrogel for Pb^{2+} is –0.055 kJ mol^{-1} K^{-1}, $\Delta S < 0$ indicates that the adsorption of Pb^{2+}at the solid–liquid interface is a reaction with reduced chaos. $\Delta G < 0$, which indicates that Pb^{2+} adsorption on PASP/SPP hydrogel is a spontaneous reaction process, the temperature continues to rise, and the absolute value of ΔG gradually decreases, indicating that the spontaneous degree of the reaction gradually decreases, which is unfavorable to the adsorption process.

Table 3
Thermodynamic parameters for the adsorption of Pb^{2+} by PASP/SPP hydrogel

T (°C)	ΔG (kJ mol^{-1})	ΔH (kJ mol^{-1})	ΔS (kJ mol^{-1} K^{-1})
30	–2.77		
40	–2.22		
50	–1.67	–19.44	–0.055
60	–1.12		
70	–0.57		

3.7. Effect of the desorption parameters on desorption capacity

3.7.1. HNO_3 concentration

As shown in Fig. 20, when the HNO_3 concentration is 0.08 mol L^{-1} the largest desorption capacity of Pb^{2+} on PASP/SPP hydrogel could achieved to 497.28 mg g^{-1}. Low concentration nitric acid solution promotes the desorption of hydrogel. H^+ and heavy metal ions attached to hydrogel form competitive adsorption on the active sites, thus increasing the desorption amount of hydrogel. High concentration nitric acid solution can inhibit desorption, and the electrostatic repulsion between excessive H^+ and heavy metal ions increases, resulting in a decrease in desorption of hydrogel [19]. Therefore, it is reasonable to choose 0.08 mol L^{-1} HNO_3 concentration.

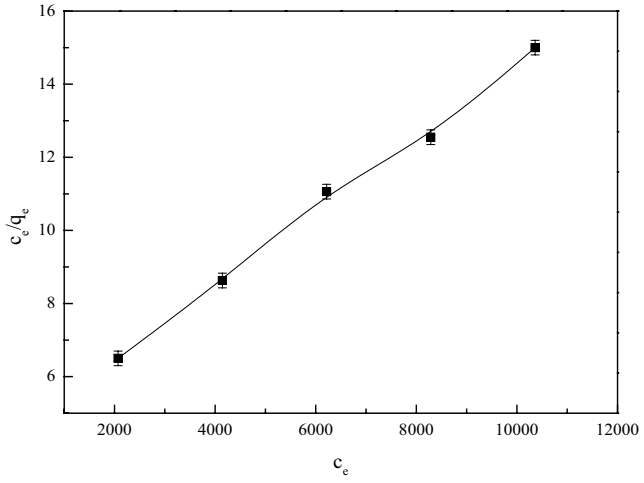

Fig. 15. Langmuir isotherm model for the adsorption of Pb^{2+} by PASP/SPP hydrogel.

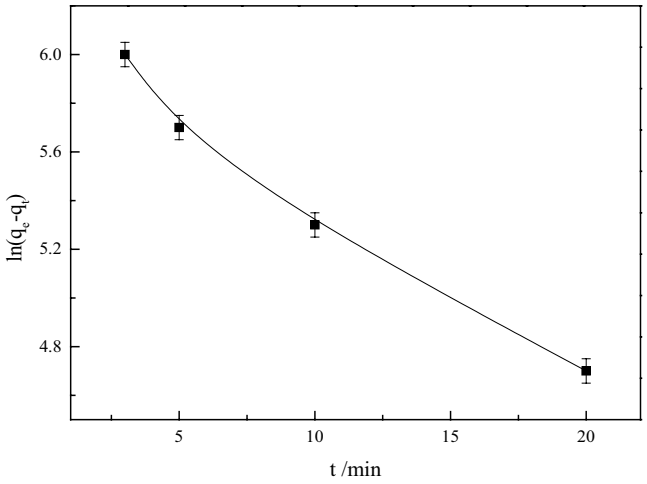

Fig. 17. Pseudo-first-order kinetic model for the adsorption of Pb^{2+} by PASP/SPP hydrogel.

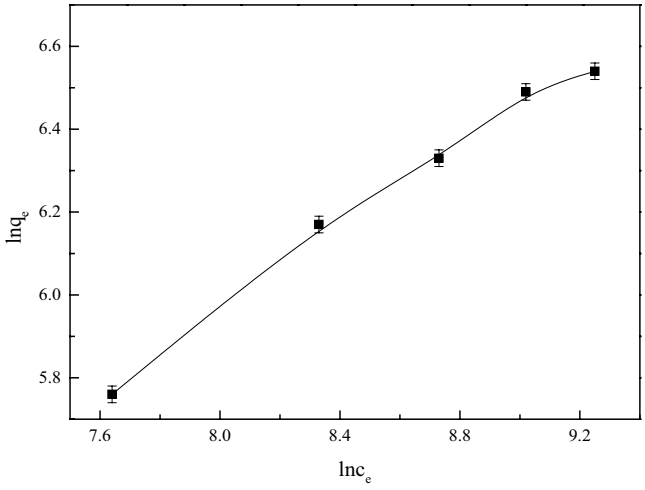

Fig. 16. Freundlich isotherm model for the adsorption of Pb^{2+} by PASP/SPP hydrogel.

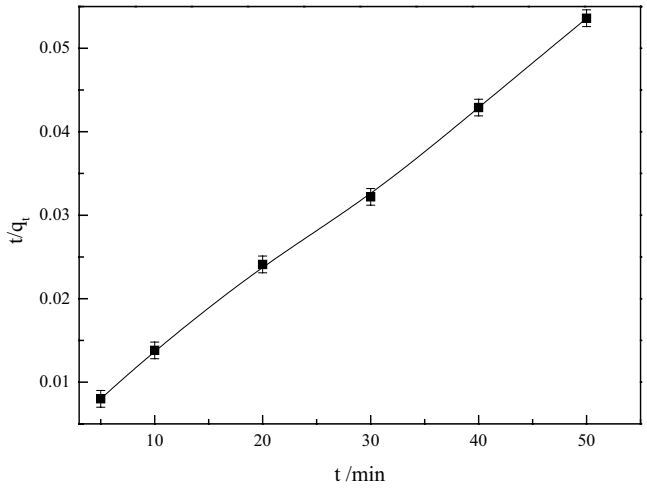

Fig. 18. Pseudo-second-order kinetic model for the adsorption of $Pb^{2+}$by PASP/SPP hydrogel.

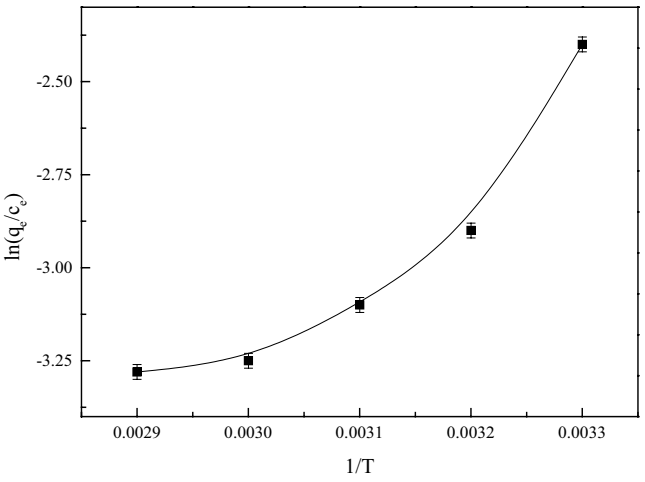

Fig. 19. Van't Hoff equation for the adsorption of Pb^{2+} by PASP/SPP hydrogel.

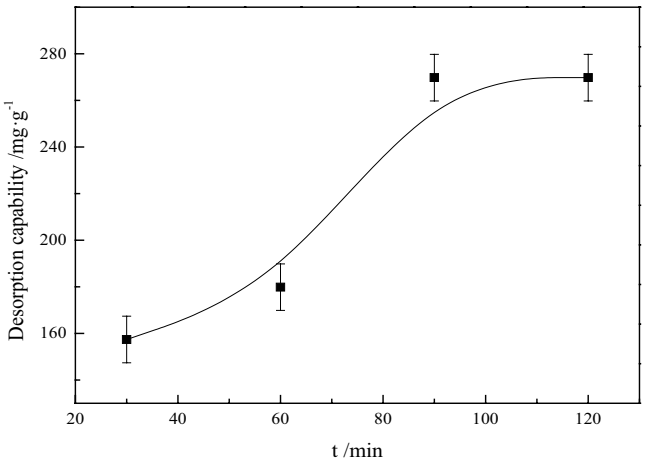

Fig. 21. Effects of the desorption time on the desorption capacity of PASP/SPP for Pb^{2+}.

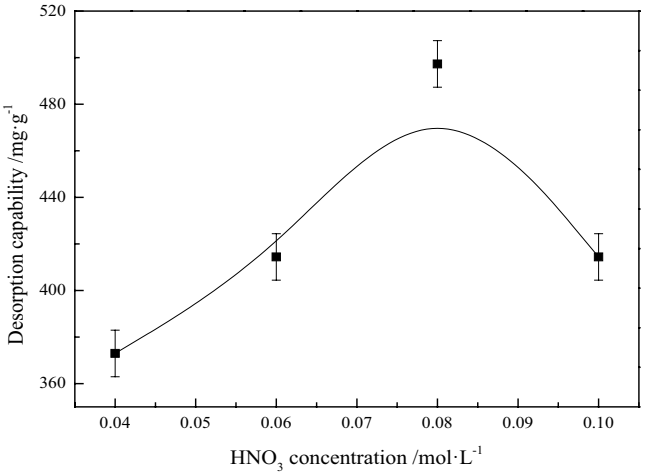

Fig. 20. Effects of the HNO_3 concentration on the desorption capacity of PASP/SPP for Pb^{2+}.

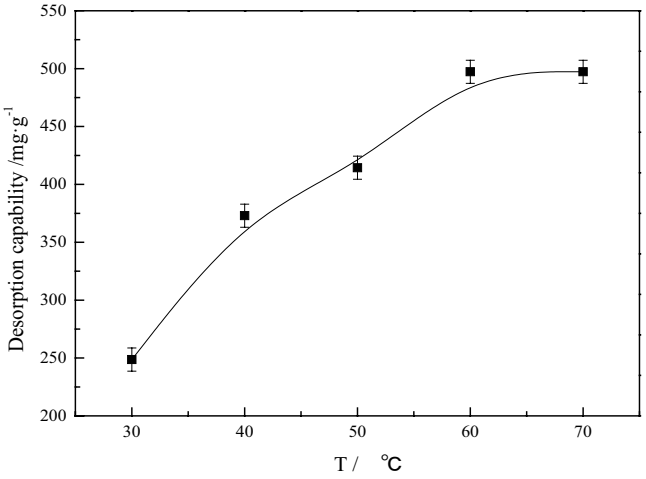

Fig. 22. Effects of the desorption temperature on the desorption capability of PASP/SPP for Pb^{2+}.

3.7.2. Desorption time

As shown in Fig. 21, when the desorption time is 90 min, the largest desorption capacity of Pb^{2+} on PASP/SPP hydrogel could achieved 497.28 mg g^{-1}. At the initial stage of desorption, the solution contains a large amount of H^+, which is easier to form competitive adsorption with heavy metal ions on adsorption sites, thus increasing the desorption amount of hydrogel. At the later stage of desorption, the concentration of H^+ gradually decreased, while the concentration of heavy metal ions in the solution gradually increased. Finally, the competitive adsorption reached equilibrium, resulting in the desorption amount remaining unchanged [20]. Therefore, desorption time of 90 min is reasonable.

3.7.3. Desorption temperature

As shown in Fig. 22, when desorption temperature is 60°C, the largest desorption capacity of Pb^{2+} on PASP/SPP hydrogel could achieved 497.28 mg g^{-1}. The activity of H^+ in the solution increases with the increase of desorption temperature, which makes it easier for H^+ to enter the microporous structure of the hydrogel and compete with the heavy metal ions adsorbed on the hydrogel for adsorption, thus the desorption amount increases continuously. With the further increase of desorption temperature, the adsorption and desorption of hydrogel form a dynamic equilibrium, so that the desorption amount remains unchanged [21]. Therefore, the desorption temperature of 60°C is more reasonable.

4. Conclusions

The results of adsorption experiments showed that, the largest adsorption capacity of PASP/SPP hydrogel to Pb^{2+} reached 936.5 mg g^{-1}. The adsorption processes of Pb^{2+} by PASP/SPP hydrogel fit very well with the Langmuir isotherm model and pseudo-second-order model. From the thermodynamic studies, it is seen that the adsorption is spontaneous, exothermic and decreased randomness. The characterization

results showed that the hydrogel surface before adsorption was loose and porous, and the hydrogel surface after adsorption became dense. XPS proved more directly that heavy metal ions were adsorbed on the hydrogel surface. The results of desorption experiments showed that, the largest desorption capacity of Pb^{2+} on PASP/SPP hydrogel could achieved 497.28 mg g^{-1}.

Funding statement

This work was financially supported by Inner Mongolia Natural Science Funds Projects (No. 2016MS0210) and the Outstanding Young Science Foundation of Inner Mongolia Agricultural University (No. 2014XYQ-12).

References

[1] J.J. Zhou, J. Zhou, R.G. Feng, Status of China's heavy metal contamination in soil and its remediation strategy, Bull. Chin. Acad. Sci., 29 (2014) 315–320 + 350.
[2] O. Amiri, H. Emadi, S.S.M. Hosseinpour-Mashkani, M. Sabet, M.M. Rad, Simple and surfactant free synthesis and characterization of CdS/ZnS core–shell nanoparticles and their application in the removal of heavy metals from aqueous solution, RSC Adv., 7 (2014) 10990–10996.
[3] J. Zhang, X.X. Cui, Z.W. Yue, X.H. Dang, B. Zhang, J. Chen, Study on adsorption properties of copper ion by salix biochar in the soil of mining area, Res. Soil Water Conserv., 25 (2018) 270–275.
[4] K. Satoshi, H. Koh, M. Rei, M. Kengo, K. Tanaka, K. Atsushi, Aorigele, Chemical composition of desert willow (*Salix psammophila*) grown in the Kubuqi Desert, Inner Mongolia, China: bark extracts associated with environmental adaptability, J. Agric. Food. Chem., 61 (2013) 12226–12231.
[5] J.X. Liu, W.H. Zou, Study on adsorption of 2,4-dichlorophenol with activated carbon made by *Salix psammophila*, New Chem. Mater., 45 (2017) 204–206 + 213.
[6] G.-L. Zhang, Y.-Z. Bao, Y.-W. Miao, Adsorption kinetics and isotherm of methylene blue on activated carbon from sandlive willow, Chem. Ind. For. Prod., 34 (2014) 129–134.
[7] F.-L. Xiao, M. Wei, J. Zhao, Advance in research of polyaspartic acid, Biomass Chem. Eng., 48 (2014) 50–55.
[8] C.Z. Geng, M.R. Tang, Progress on polyaspartic acid as an environmental friendly water treatment agent, Appl. Chem. Ind., 44 (2105) 1350–1353.
[9] B. Sun, Z.T. Mi, S.X. Shao, Preparation of polyaspartate hydrogel using microwave technique and its Pb^{2+} binding behaviour, Petrochem. Technol., 33 (2004) 1168–1172.
[10] M.H. Ye, L. Wang, Preparation and absorption properties of polyaspartic acid/lignocellulose hydrogels, Acta Materiae Compositae Sinica, 33 (2016) 2094–2103.
[11] B. Peng, C. Shen, Q. Meng, Swelling factors of DA-P123 hydrogel and its application in heavy metal ions removal from aqueous solutions, J. Chem. Eng. Chin. Univ., 31 (2017) 1426–1432.
[12] K. Kabiri, H. Omidian, M.J. Zohuriaan-Mehr, S. Doroudiani, Superabsorbent hydrogel composites and nanocomposites: a review, Polym. Compos., 32 (2011) 277–289.
[13] Y.Y. Zhao, S.T. Jiang, J.Q. Zhou, P. Shao, Research on grafting of acrylamide onto sweet potato starch initiated by $KMnO_4$, J. Hefei Univ. Technol., 11 (2004) 1391–1395.
[14] J. Zhang, C.H. Mao, X.L. Chen, Synthesis of poly(aspartic acid) superabsorbent polymer in aqueous solution, China Plast. Ind., 41 (2013) 13–16 + 26.
[15] W.Y. Liu, L.Z. Yang, M. Yu, M. Sun, Preparation of poly(acrylate-acrylamide) hydrogel and its adsorption performance to heavy metal ions, Chin. J. Anal. Chem., 44 (2016) 707–715.
[16] X.D. Liu, Y. Li, J. Xiong, Y.F. Sun, F.Z. Tan, Adsorption ability of modified corn straw for Cu^{2+}, J. Dalian Polytech. Univ., 37 (2018) 100–104.
[17] A. Salama, K.R. Shoueir, H.A. Aljohani, Preparation of sustainable nanocomposite as new adsorbent for dyes removal, Fibers Polym., 18 (2017) 1825–1830.
[18] R. Karthik, S. Meenakshi, Removal of Pb(II) and Cd(II) ions from aqueous solution using polyaniline grafted chitosan, Chem. Eng. J., 263 (2015) 168–177.
[19] C.L. Zhang, X.M. Hu, Y. Zhao, L. Su, Adsorption behavior of anionic dyes onto magnetic chitosan derivatives, Environ. Sci., 36 (2015) 221–226.
[20] Q. Li, J.D. Cui, D.D. Lu, W.H. Li, Desorption and regeneration properties for heavy metal ions of CD/PAN nanofiber membranes, Dyeing Finish., 44 (2018) 11–16.
[21] D.Y. Tang, Z. Zheng, D.H. Su, C.H. Gu, P.G. Zhou, K. Lin, Adsorption of *p*-nitrophenol from wastewater by activated carbon fiber and its desorption, Chin. J. Environ. Eng., 1 (2006) 98–101.